Journal of Industrial and Engineering Chemistry 113 (2022) 373–379

Contents lists available at ScienceDirect

Journal of Industrial and Engineering Chemistry

journal homepage: www.elsevier.com/locate/jiec

Nanofibrous membranes with antibacterial and thermoregulatory functions fabricated by coaxial electrospinning

Zhuofan Qin [a], Shuoshuo Wang [a], Lina Wang [a], Juming Yao [a], Guocheng Zhu [a], Baochun Guo [b], Jiri Militky [c], Mohanapriya Venkataraman [c], Ming Zhang [a,*]

[a] Zhejiang-Czech Joint Laboratory of Advanced Fiber Materials, Zhejiang Sci-tech University, China
[b] Department of Polymer Materials and Engineering, South China University of Technology, Guangzhou 510640, China
[c] Department of Material Engineering, Faculty of Textile Engineering, Technical University of Liberec, Czech Republic

ARTICLE INFO

Article history:
Received 29 April 2022
Revised 31 May 2022
Accepted 7 June 2022
Available online 14 June 2022

Keywords:
Antibacterial properties
Phase change material
Coaxial electrospinning

ABSTRACT

Bacteria, viruses, and temperatures change can affect the preservation of food and medicines, so it is necessary to develop an intelligent textile for antibacterial and thermal regulation. In this paper, we used coaxial electrospinning technology to achieve antibacterial thermo-regulating intelligent textiles. The polyacrylonitrile (PAN)/curcumin is the sheath, and n-octadecane is the core. The composite fiber has excellent comprehensive properties. When the curcumin concentration is 10 wt%, the antibacterial effect is the best, and the bacteriostatic rate is 100%. When the core feed rate is 0.25 mL/h, the latent heat can reach 123.94 J/g. The multifunctional textiles have potential application value in the clothing fabrics, preservation and storage quality of functional foods, biomedical products, and other fields.

Introduction

Since bacteria, viruses, and other microorganisms widely exist in nature such as food, water, and air, they pose a huge threat to human health [1–5]. Therefore, it is crucial to develop a low-cost [6], high-performance [7,8] antibacterial material. Among many microorganisms, E. coli and S. aureus are widely present in various foods and can multiply rapidly [9,10]. They can cause severe food poisoning and bacterial infections and are the most harmful human pathogens, so we should suppress their presence [11–14]. Therefore, textiles with antibacterial functions have attracted attention because they can protect people from bacteria.

Curcumin is a yellow pigment extracted from the ginger plant turmeric. [15,16] It is one of the most popular natural food colorings in the world [17]. It has the advantages of being natural [18], green [19], and has pharmacological effects such as antibacterial [17,20,21], anti-inflammatory [22], and antiviral [23]. Studies have shown that curcumin attacks the permeability of cell membranes and cell walls to rupture cells, resulting in a bactericidal effect. Many people use curcumin as an antibacterial agent and study antibacterial fiber membranes [24]. Wang et al. used curcumin, konjac glucomannan, and zein to prepare nanofiber films with great antibacterial effects [25]. Yakub et al. prepared antibacterial nanofibrous membranes with curcumin and polylactic acid [26].

Although antibacterial fibers can protect food, medicine, and other substances from bacteria, temperature changes will shorten their shelf life, so it is necessary to make antibacterial fiber have the function of thermo-regulation. However, there are few reports on antibacterial membranes with thermo-regulation functions so far. Phase change material (PCM) is something that absorbs and releases latent heat by changing the state of matter to maintain a constant temperature [27,28]. Heat is absorbed and stored during melting and released during crystallization. PCMs have been used widely in clothing, food packaging, and other fields [29–31]. The n-octadecane is a typical organic solid–liquid PCM. The advantages of this material include low price, low corrosiveness, good stability, high latent heat storage capacity, and an appropriate phase transition temperature [32–34]. However, PCMs are easily leaky when repeatedly melted and cooled, limiting their practical applications [31,35–37]. The coaxial electrospinning method can solve this problem very well [34,38]. This method can directly add PCMs to nanofibers through coaxially arranged spinnerets to prepare core-sheath structure nanofibers with small pore size, high porosity, high specific surface area, and stable thermal properties [39–42]. Using this method, antibacterial and thermo-regulation functions can be well integrated into the fabric. With the development

* Corresponding author.
E-mail address: zhangming@zstu.edu.cn (M. Zhang).

https://doi.org/10.1016/j.jiec.2022.06.012

of coaxial electrospinning technology, core-sheath structure nanofibers have been used widely in aerospace, clothing, thermal regulation of electronic components, and other fields [37,43–46].

In this paper, we prepared composite nanofibers with antibacterial and thermo- regulation functions by coaxial electrospinning technology. The advantages of PAN as a polymer substrate include thermal stability, mechanical properties, and great spinnability [47–50]. The antibacterial agent was curcumin, and the PCM used n-octadecane. Add curcumin to PAN to prepare nanofibers with antibacterial function. The n-octadecane was encapsulated in the nanofibers to endow the fibers with the thermal regulation function. The effect of curcumin concentration on the bacteriostatic rate and the effect of the core feed rate on the encapsulation rate of n-octadecane was also systematically discussed. Antibacterial thermo-regulation fibers with excellent comprehensive properties were prepared successfully. The multifunctional nanofiber membrane has great application potential in the field of food and biomedicine.

Experimental procedure

Materials

Polyacrylonitrile (PAN, Mw = 140,000) was purchased from Sinopec Shanghai Petrochemical Co. Ltd. China. NaCl and N, N-dimethyl formamide (DMF) were purchased from Hangzhou Gaojing Fine Chemical Industry Co. Ltd. Petroleum ether (AR, bp 90–120 °C) and n-octadecane (99%, melting temperature is around 28 °C) were purchased from Aladdin Chemistry Co., Ltd. Curcumin (AR, Mw = 368.38 Da) was purchased from Ron's reagent. Agar powder and peptone were purchased from Hangzhou Baisi Biotechnology Co., Ltd. Yeast infusion powder was purchased from Macklin Biochemical Technology Co., Ltd.

Methods

To obtain the sheath solution, 12 wt% PAN and different concentrations of curcumin (0 wt%, 4 wt%, 6 wt%, 8 wt%, 10 wt%) were added to DMF and magnetically stirred for 12 h. The core material is n-octadecane. The applied high voltage and the distance from the tip to the collector were 25 kV and 18 cm, respectively. The sheath feed rate was 0.6 mL/h, and the core feed rate was 0.05 mL/h, 0.10 mL/h, 0.15 mL/h, 0.20 mL/h, 0.25 mL/h respectively.

The stainless-steel double spinneret consisted of an internal spinneret (outer/inner diameters were 0.72/0.41 mm) and an external spinneret (outer/inner diameters were 1.49/1.01 mm). Use the heating unit and dehumidifier inside the electrospinning machine to keep the ambient temperature and the relative humidity at 40 °C and 30%, respectively.

Characterizations

Use the FE-SEM (ULTRA55, Zeiss) to observe the morphology of the nanofibers, the acceleration voltage is 3 kV. All the samples are presoaked in petroleum ether for 24 h and then coated with a thin layer of gold. Use ImageJ software to measure the diameters of 30 random fibers, and calculate their average values. The core-sheath structure of the nanofibers is investigated by FE-TEM (JEM-2100, JOEL) at an accelerating voltage of 200 kV. Nanofibers are deposited directly on 400 mesh carbon-coated copper grids, and then the copper grids are presoak in petroleum ether for 24 h to remove. Measured tensile properties by multifunctional mechanical tester (KES-G1) with a tensile rate of 0.1 cm/s at 25 °C. The samples are cut into small pieces of 0.5 × 2 cm, and the thickness was accurate to 1 μm. DSC (Q2000) is carried out in nitrogen flow with a heating and cooling rate of 10 K/min. Samples are heated from 5 to 50 °C and cooled from 50 to 5 °C. Characterizing the chemical structure of nanofibers by FTIR (Nicolet Nexus-560, Madison, WI, USA). The spectral range is 350–4000 cm^{-1}. Through TGA (L81/1750, LINSEIS Company, Germany), we obtained the thermal stability and decomposition properties of the fiber membrane. Using an improved modified AATCC 100–1999 method [51,52], E. coli and S. aureus were model microorganisms. The bacteriostatic reduction rate (BR) of the microorganism is calculated as follows:

$$BR = B\text{-}A/B \times 100\%, \quad (1)$$

A and B are the surviving microorganisms (CFU)/mL on the agar plates of the experimental group and the control group after 24 h. The procedure is repeated three times.

Results and discussion

A new type of antibacterial thermo-regulated composite fiber was prepared by electrospinning technology. As shown in Fig. 1, connect the core and sheath solution with the stainless-steel double spinneret. A suitable high voltage was applied to the needle, and the electric field force stretched the solution to form a jet, and the fiber was obtained on the collector finally. This method can encapsulate the PCM in nanofiber and form core-sheath structure nanofiber. The polymer sheath can maintain the stability of the fiber shape, provide mechanical strength, and effectively prevent PCM leaks during the transition between solids and liquids.

Curcumin, which has antibacterial properties, was added to the sheath solution to make the antibacterial fiber. Fig. 2 shows the SEM images of PAN/Cur fibers with different curcumin concentrations. As seen in the SEM images, the surface of pure PAN fiber was smooth and had a uniform cylindrical shape. After adding curcumin to PAN, the fiber morphology did not change significantly. The fiber surface was still smooth without particles or beads, indicating that the curcumin was dissolved in the sheath solution completely. Fig. 3 was the average diameter of the fiber. With the increase in curcumin concentration, the fiber's average diameter also increases. The possible reason was that with the curcumin concentration increase, and the viscosity of the solution increases, the molecular chain entanglement also increases, so the PAN/Cur fiber average diameter increases.

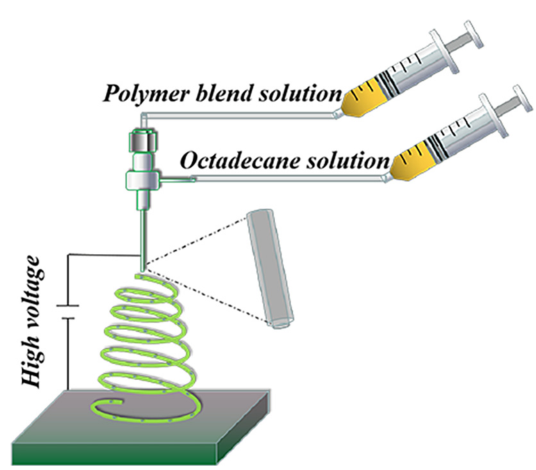

Fig. 1. Schematic diagram of coaxial electrospinning.

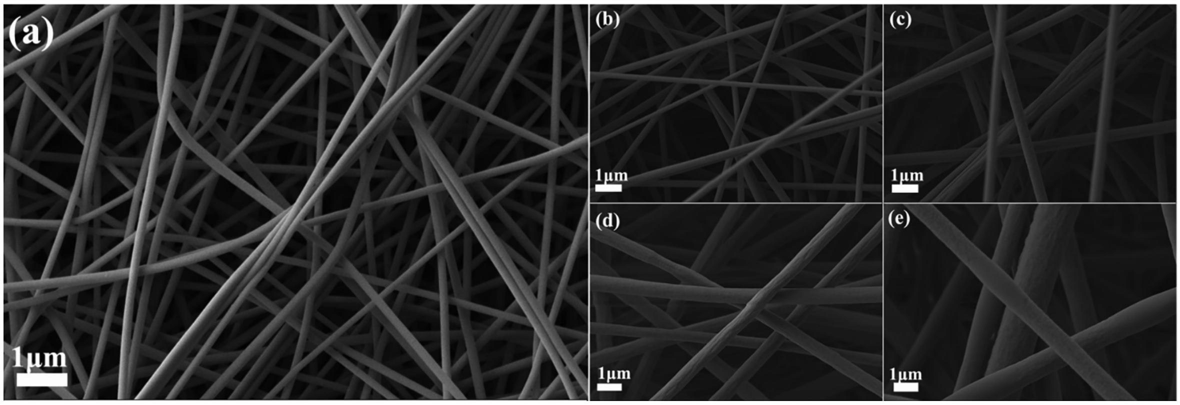

Fig. 2. SEM images of PAN/Cur fiber with curcumin concentration of (a) 0 wt%, (b) 4 wt%, (c) 6 wt%, (d) 8 wt%, (e) 10 wt%.

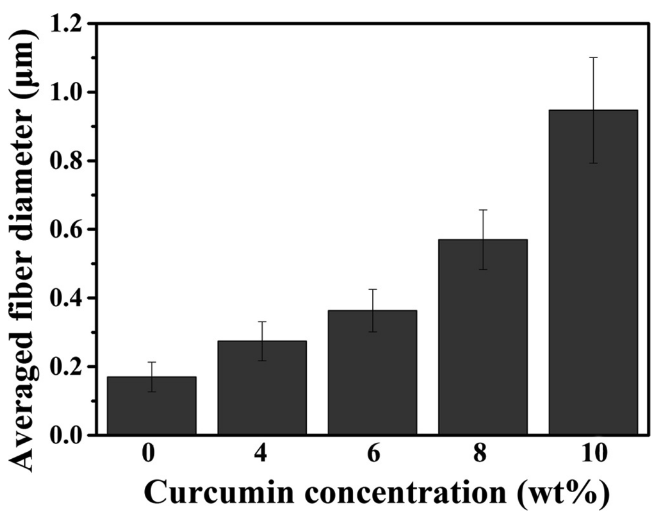

Fig. 3. The average diameters of PAN/Cur nanofibers containing different curcumin concentrations.

Test the antibacterial properties of the fiber. As shown in the figure, Fig. 4 shows the antibacterial effect of the fibrous membrane on E. coli and S. aureus after adding different concentrations of curcumin. Fig. 5 was the bacteriostatic rate of the fibrous membrane. The fibrous membrane without curcumin has no antibacterial effect, and Petri dishes were overgrown with colonies. With the increase of curcumin concentration, the antibacterial effect of the fibrous membrane was getting better and better. When the curcumin concentration was 10 wt%, the antibacterial effect was the best, there were no colonies on the petri dish, and the bacteriostatic rate of the fibrous membrane against E. coli and S. aureus was 100%. Comparing the antibacterial effect of the fibrous membrane on E. coli and S. aureus, curcumin has a far better antibacterial effect on S. aureus than E. coli. This phenomenon may be related to the composition and structure of the cell wall. The cell wall of E. coli is a phospholipid membrane, and the cell wall of S. aureus is a peptidoglycan layer. Curcumin is more likely to combine with the peptidoglycan layer to destroy the cell structure, so the fiber has a better bacteriostatic effect on S. aureus [53].

Encapsulating n-octadecane in PAN/Cur fibers to prepare core-sheath nanofibers. Fig. 6 shows the SEM image of PAN/Cur@Oct

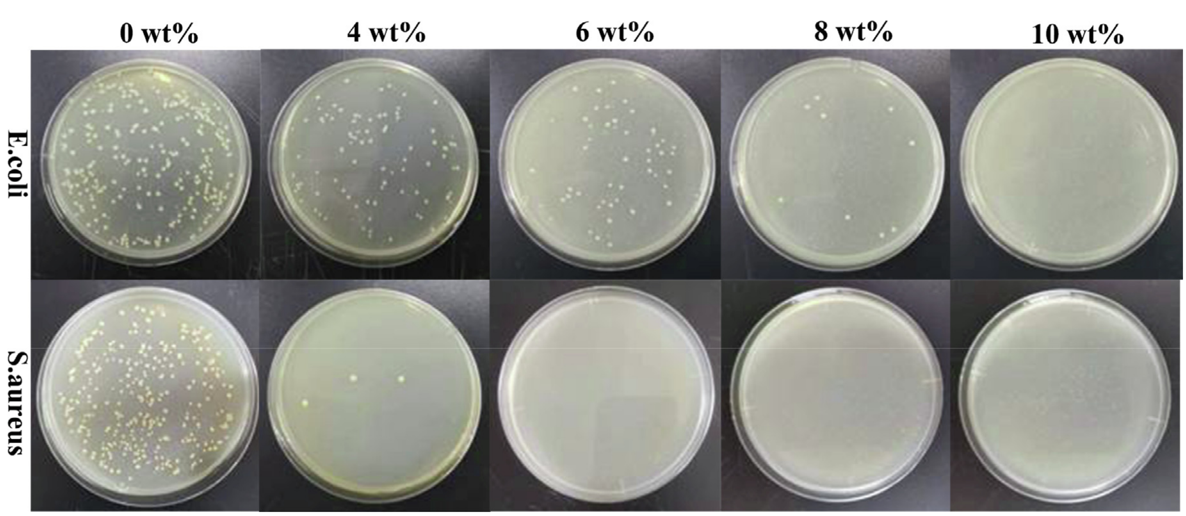

Fig. 4. Optical image of antibacterial effect of the fiber membrane against E. coli and S. aureus.

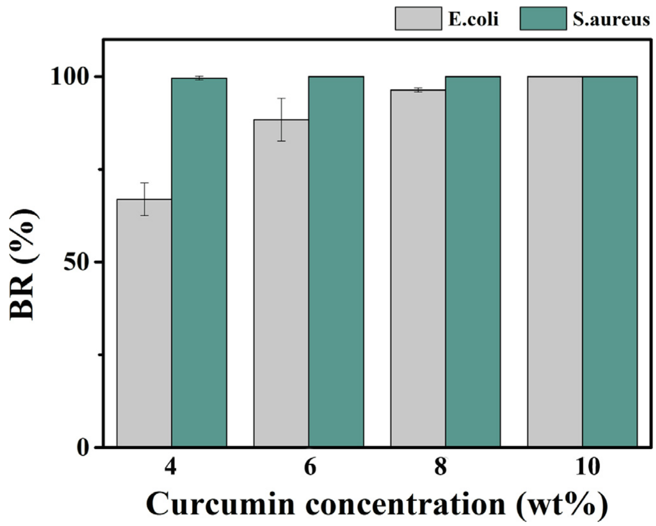

Fig. 5. Bacteriostatic rate of the fiber membrane against E. coli and S. aureus.

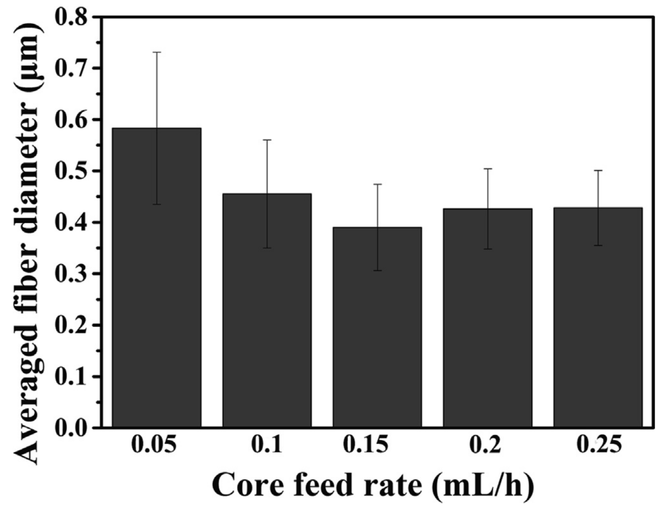

Fig. 7. The average diameter of PAN/Cur@Oct nanofibers at different core feed rate.

fibers. The morphology of PAN/Cur@Oct fibers did not change much compared with PAN/Cur fibers. The surface of the PAN/Cur@-Oct fiber was smooth and showed a uniform cylindrical shape, indicating that the n-octadecane was encapsulated inside the fibers rather than sprayed simply on the surface. Fig. 7 shows the average diameter of PAN/Cur@Oct fiber. Changing the core feed rate, the average diameter of the composite fiber did not change much, indicating that the fiber's average diameter was independent of the core feed rate.

Fig. 8 was the DSC curve of PAN/Cur@Oct fiber, and Table 1 was the corresponding data. As the core feed rate increases, the latent heat value of the nanofiber also increases. The latent heat value cannot be increased infinitely. The latent heat value finally reaches its highest point when the core feed rate was 0.25 mL/h, and this condition was the PAN/Cur fiber maximum encapsulation rate. Calculation of the n-octadecane loading in nanofiber can be done by the formula:

$$\text{Encapsulation ratio } (\%) = \triangle H_{m,PCM/Sheath} \ / \ \triangle H_{m,PCM} \times 100\%, \quad (2)$$

where $\triangle H_{m,PCM/Sheath}$ and $\triangle H_{m,PCM}$ represent the melting enthalpy values of nanofibers and pure n-octadecane. The highest latent heat value of PAN/Cur@Octa was 123.94 J/g, while n-octadecane was 255.03 J/g [46]. Therefore, the n-octadecane encapsulation rate was 48.6%.

Fig. 9 displays the core-sheath structure of the nanofiber. At the same core feed rate, the polymer sheath with curcumin has a higher n-octadecane loading than the pure PAN polymer sheath. The possible reason was that after adding curcumin to the polymer, the viscosity of the solution increases, and the encapsulation efficiency of n-octadecane also increases.

Fig. 10 demonstrates the antibacterial effect of the fiber after encapsulating n-octadecane. After encapsulating n-octadecane in PAN/Cur fiber, the bacteriostatic rate of the PAN/Cur@Oct nanofibrous membrane was 100%. It indicates that the encapsulated n-octadecane had no effect on the antibacterial effect of the fibers, and the composite fiber had good antibacterial properties.

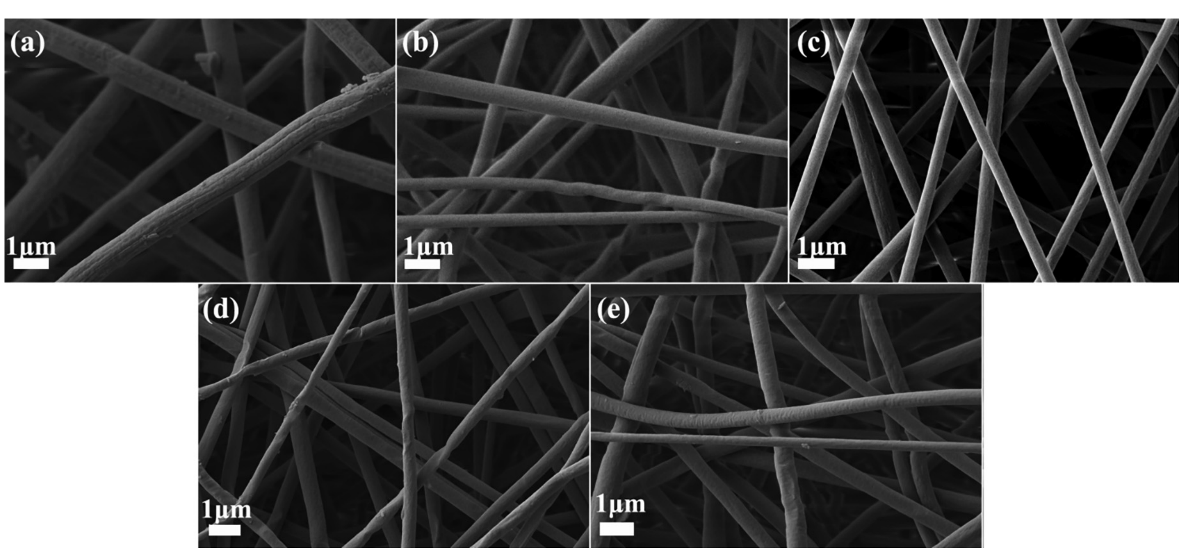

Fig. 6. The SEM images of PAN/Cur@Oct nanofibers with different core feed rates: (a) 0.05 mL/h, (b) 0.10 mL/h, (c) 0.15 mL/h, (d) 0.20 mL/h, (e) 0.25 mL/h.

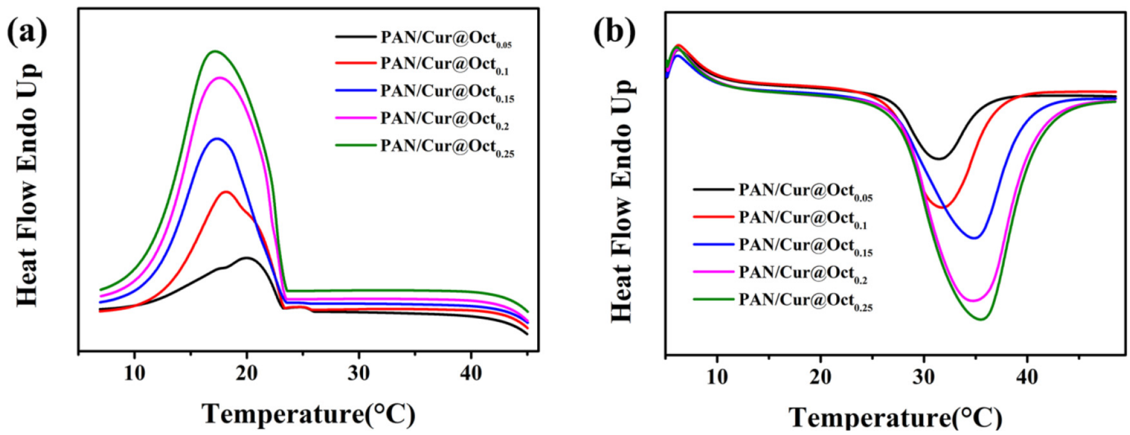

Fig. 8. DSC curves of PAN/Cur@Oct fibers with core feed rate of 0.05 mL/h, 0.1 mL/h, 0.15 mL/h, 0.2 mL/h, 0.25 mL/h (a) heating stage, (b) cooling stage.

Table 1
DSC data of PAN/Cur@Oct fibers and n-octadecane.

Samples	Core feed rate (mL/h)	T_m (°C)	$\triangle H_m$ (J/g)	T_c (°C)	$\triangle H_c$(J/g)
PAN/Cur@Oct	0.05	19.96	23.98	31.40	23.93
	0.1	18.12	52.11	31.70	50.69
	0.15	17.37	73.86	34.82	71.81
	0.2	17.61	109.38	34.62	106.47
	0.25	17.20	123.94	35.48	120.44
n-octadecane		28.36	255.03	19.76	251.31

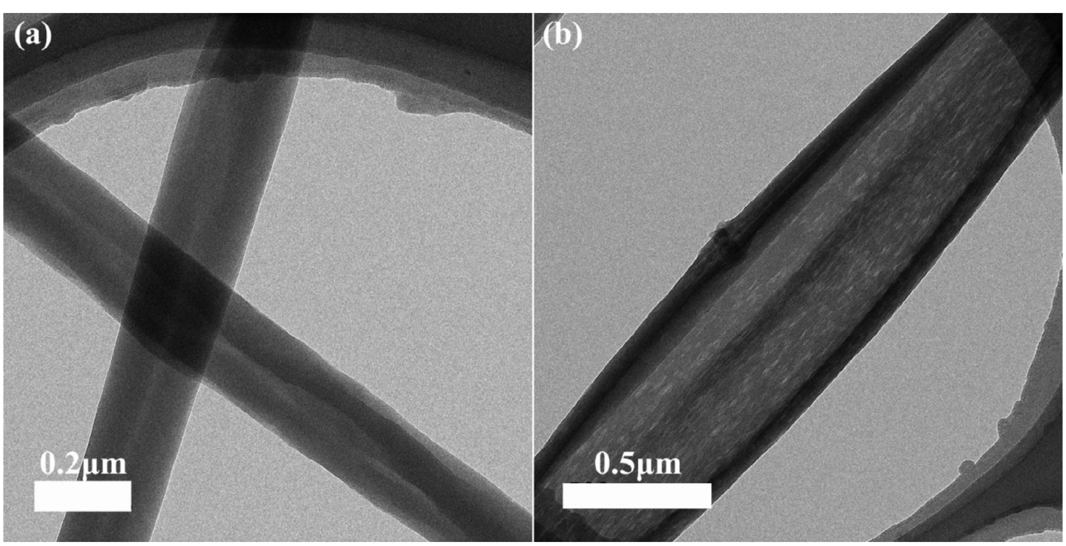

Fig. 9. TEM images of (a) PAN@Oct, (b) PAN/Cur@Oct fibers with the sheath feed rate of 0.6 mL/h and the core feed rate of 0.25 mL/h.

Thermal stability of PAN, curcumin, n-octadecane, and PAN/Cur@Oct were evaluated using thermogravimetric analysis (TGA). Fig. 11 shows the relationship between sample temperature and percent weight loss. The results show that n-octadecane initially decomposes at about 120 °C and completely decomposes at about 250 °C. Curcumin initially decomposes at around 250 °C, and PAN initially decomposes at about 310 °C. There are two stages of decomposition of the PAN/Cur@Oct fibers. In the first stage, n-octadecane was thermal decomposed, and the mass loss was the amount of n-octadecane loaded on the nanofiber. The second stage was the thermal decomposition of curcumin and PAN. The decomposition temperature of n-octadecane in the composite fibers was increased, indicating that the core-sheath fiber can increase the decomposition temperature of PCMs and improve the thermal stability of PCMs [46].

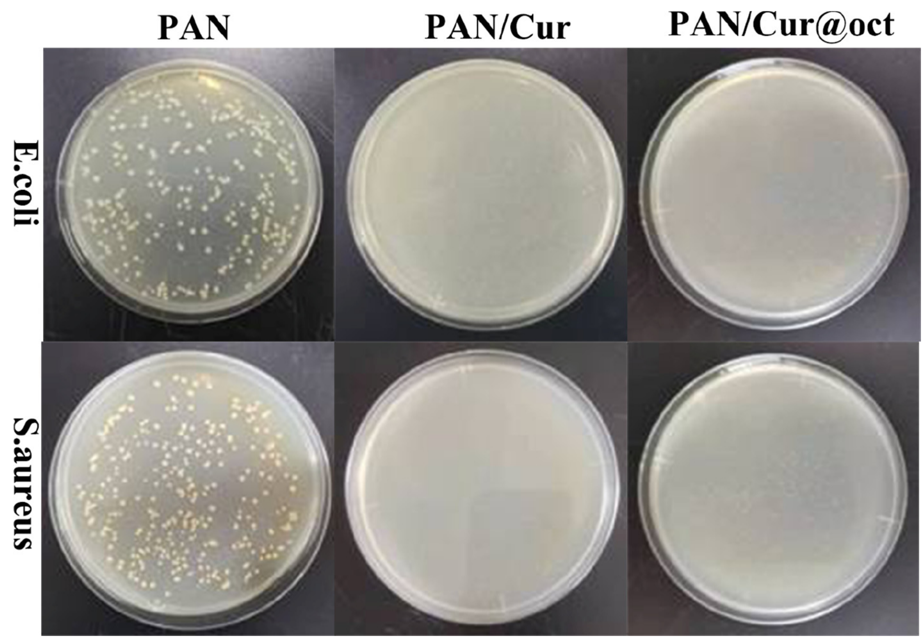

Fig. 10. Optical image of antibacterial effect of PAN, PAN/Cur, and PAN/Cur@Oct fibers against E. coli and S. aureus.

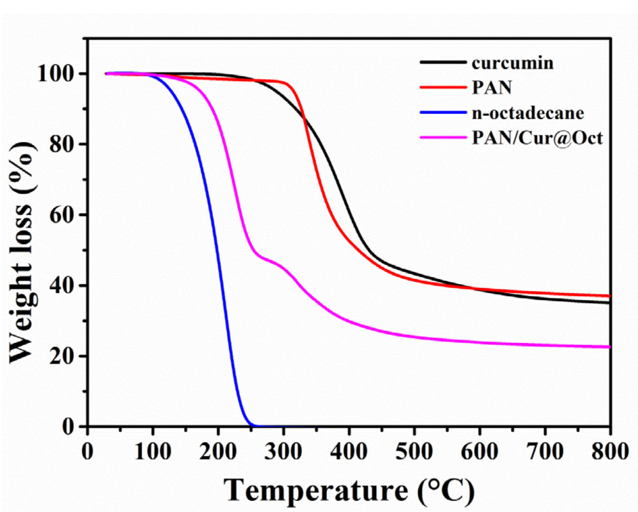

Fig. 11. Thermogravimetric analysis curves of curcumin, PAN, n-octadecane, PAN/Cur@Oct.

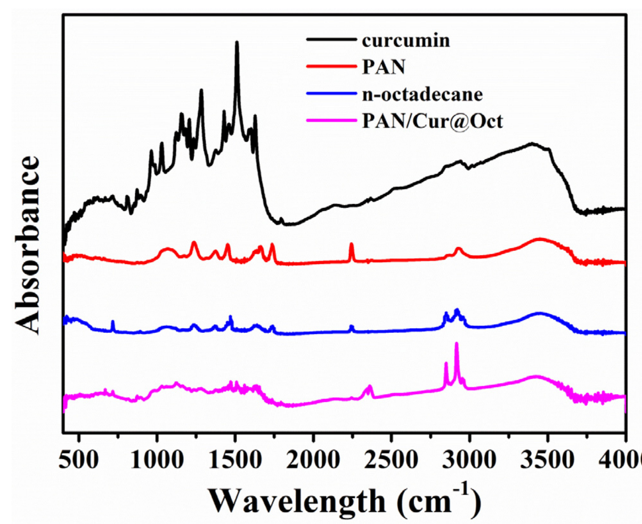

Fig. 12. Fourier transform infrared spectra of curcumin, PAN, n-octadecane, PAN/Cur@Oct.

Fig. 12 was the infrared spectrum of curcumin, PAN, n-octadecane, PAN/Cur@Oct. The infrared peak of curcumin at 3501 cm^{-1} and 1626 cm^{-1} corresponds to the stretching vibration peak of phenolic (–OH) and carbonyl (C=O). The peak at 1800–1650 cm^{-1} was the carbon-based region [25]. In the spectrum of n-octadecane, 2922 cm^{-1} and 2853 cm^{-1} represent the C–H symmetric stretching vibrations in the methyl and methylene groups. The 1469 cm^{-1} was the characteristic absorption peak of the C–H bending vibration. The absorption peak at 717 cm^{-1} was the long carbon chains [38,46]. Stretching vibrations of the nitrile group (–CN) were found at 2237 cm^{-1} for the PAN film [48]. The spectrum of composite fiber shows all characteristic absorption peaks of the core and sheath and does not form new absorption bands. It indicates that the PAN/Cur@Oct fiber was coated with n-octadecane successfully and had no chemical reaction.

Fig. 13 shows the stress–strain curve of nanofibrous fabrics. The mechanical strength of pure PAN fibers was the best. After adding curcumin to PAN, the elongation of the fibers did not change much, but the mechanical strength decreased slightly. The likely reason was that curcumin destroys the internal connections of the fibers. After encapsulation of n-octadecane in the PAN/Cur sheath, the mechanical strength decreased slightly, and the elongation of the fiber decreased a lot. Because it was the loaded brittle n-octadecane weakens the mechanical properties of the nanofibers [38,46].

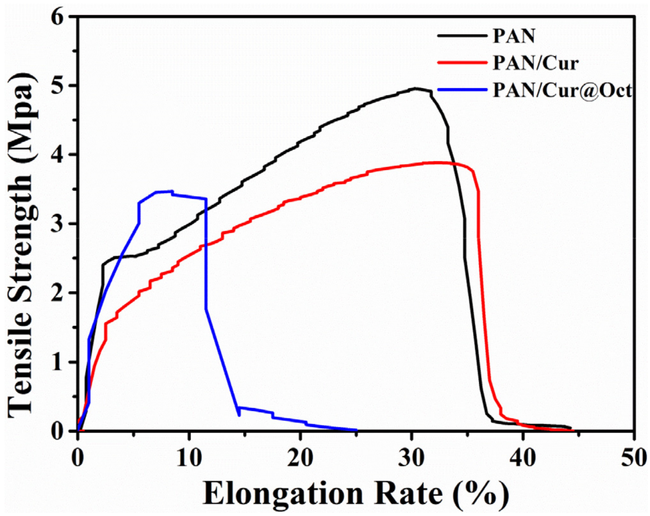

Fig. 13. Stress–strain curves of PAN, PAN/Cur, PAN/Cur@Oct fiber.

Conclusions

In summary, we prepared smart nanofibrous membranes with antibacterial and thermal regulation functions by coaxial electrospinning. Adding curcumin to polyacrylonitrile imparts excellent antibacterial function to the fiber. The TEM image shows that PAN/Cur@Oct fiber has a core-sheath structure, and the polymer coats n-octadecane successfully, giving the fiber thermal regulation function. After the polymer was loaded with n-octadecane, the bacteriostatic rate was still 100%, indicating that the composite fiber had good comprehensive properties. Therefore, this work provides strong support for the application study of multifunctional textiles.

Declaration of Competing Interest

The authors declare that they have no known competing financial interests or personal relationships that could have appeared to influence the work reported in this paper.

Acknowledgement

This study was supported by the 111 Project (D21011), China education association for international 278 exchange (Grant No.: 202020), and Zhejiang Provincial Key Research and Development Program (2022C03093).

References

[1] W. Yu, X. Li, J.X. He, Y.K. Chen, L.Y. Qi, P.P. Yuan, et al., J. Colloid Interface Sci. 584 (2021) 164–173.
[2] H. Li, X. Chen, W. Lu, J. Wang, Y. Xu, Y. Guo, Nanomaterials 11 (2021).
[3] F. Topuz, T. Uyar, Food Res. Int. 130 (2020).
[4] S. Homaeigohar, A.R. Boccaccini, Acta Biomater. 107 (2020) 25–49.
[5] C.R. Sahoo, J. Sahoo, M. Mahapatra, D. Lenka, P.K. Sahu, B. Dehury, et al., Arabian J. Chem. 14 (2021).
[6] A. Babapoor, G. Karimi, S.I. Golestaneh, M.A. Mezjin, Appl. Therm. Eng. 118 (2017) 398–407.
[7] Y. Cai, S. Ma, in Progress in the Study of Antibacterial Fibers, pp. 103-106, Dalian, Peoples R China (2013).
[8] R.F. Zhao, P.F. Tan, Y.T. Han, F. Yang, Y.D. Shi, P.X. Zhu, et al., Polymers 13 (2021).
[9] S. Wang, J. Yao, B. Zhou, J. Yang, M.T. Chaudry, M. Wang, et al., J. Food Prot. 81 (2018) 68–78.
[10] Y. Zhang, X. Liu, Y. Wang, P. Jiang, S. Quek, Food Control 59 (2016) 282–289.
[11] X. Zhang, M. Qin, M. Xu, F. Miao, C. Merzougui, X. Zhang, et al., Eur. Polym. J. 146 (2021).
[12] S. Saidin, M.A. Jumat, N.A.A.M. Amin, A.S.S. Al-Hammadi, Mater. Sci. Eng. C 118 (2021).
[13] Y. Wang, Y. Yang, Y. Shi, H. Song, C. Yu, Adv. Mater. 32 (2020).
[14] L.-E. Shi, Z.-H. Li, W. Zheng, Y.-F. Zhao, Y.-F. Jin, Z.-X. Tang, Food Addit. Contamin. Part A 31 (2014) 173–186.
[15] R. Sedghi, A. Shaabani, Polymer 101 (2016) 151–157.
[16] H.T. Bui, O.H. Chung, J. Dela Cruz, J.S. Park, Macromol. Res. 22 (2014) 1288–1296.
[17] E. Schraufstatter, H. Bernt, Nature 164 (1949) 456.
[18] C. Dai, J. Lin, H. Li, Z. Shen, Y. Wang, T. Velkov, et al., Antioxidants 11 (2022).
[19] F.M. Raduly, V. Raditoiu, A. Raditoiu, V. Purcar, Coatings 11 (2021).
[20] S.Z. Moghadamtousi, H.A. Kadir, P. Hassandarvish, H. Tajik, S. Abubakar, K. Zandi, Biomed Res. Int. 2014 (2014).
[21] D. Zheng, C. Huang, H. Huang, Y. Zhao, M.R.U. Khan, H. Zhao, et al., Chem. Biodivers. 17 (2020).
[22] S.F. Nabavi, M. Daglia, A.H. Moghaddam, S. Habtemariam, S.M. Nabavi, Compr. Rev. Food Sci. Food Saf. 13 (2014) 62–77.
[23] M.C. Albuquerque de Oliveira, F.A. Gomes da Silva, M.M. da Costa, N. Rakov, H. P. de Oliveira, Adv. Fiber Mater. 2 (2020) 256–264.
[24] A. Dl, A. Az, B. Bkt, A. Yt, C. Ssh, D. Zz, E. Sla, E.J.F.C. Jha, 361.
[25] L. Wang, R.J. Mu, Y. Li, L. Lin, J.P.J.L.-F. Sci., Technol., (2019).
[26] G. Yakub, A. Toncheva, N. Manolova, I. Rashkov, D. Danchev, V. Kussovski, J. Appl. Polym. Sci. 133 (2016).
[27] S.-X. Sun, R. Xie, X.-X. Wang, G.-Q. Wen, Z. Liu, W. Wang, et al., J. Mater. Sci. 50 (2015) 5729–5738.
[28] C.V. Do, N. Thuy, T. Thi, J.S. Park, Korean J. Chem. Eng. 30 (2013) 1403–1409.
[29] Y. Lu, X. Xiao, Y. Zhan, C. Huan, S. Qi, H. Cheng, et al., ACS Appl. Mater. Interfaces 10 (2018) 12759–12767.
[30] M. Kenisarin, K. Mahkamov, Renew. Sustain. Energy Rev. 11 (2007) 1913–1965.
[31] C. Chen, L. Wang, Y. Huang, Polymer 48 (2007) 5202–5207.
[32] Z. Qin, L. Yi, S. Wang, L. Wang, J. Yao, G. Zhu, et al., Polymer 233 (2021).
[33] L. Yi, Y. Wang, Y. Fang, M. Zhang, J. Yao, L. Wang, et al., RSC Adv. 9 (2019) (1851) 21844–121842.
[34] F. Haghighat, S.A.H. Ravandi, M.N. Esfahany, A. Valipouri, J. Mater. Sci. 53 (2018) 4665–4682.
[35] L. Zhao, J. Luo, Y. Li, H. Wang, G. Song, G. Tang, J. Appl. Polym. Sci. 134 (2017).
[36] Y. Wu, C. Chen, Y. Jia, J. Wu, Y. Huang, L. Wang, Appl. Energy 210 (2018) 167–181.
[37] C. Chen, Y. Zhao, W. Liu, Renew. Energy 60 (2013) 222–225.
[38] S. Wang, L. Yi, L. Wang, J. Yao, J. Militky, M. Venkataramam, et al., Polymer 228 (2021).
[39] M. Cudlinova, L. Vyslouzilova, P. Novak, Tanger, in: Coaxial Electrodes for Electrospinning, pp. 457-462, Brno, Czech Republic (2014).
[40] B. Pant, M. Park, S.-J. Park, Pharmaceutics 11 (2019).
[41] Q. Liu, J. Zhu, L. Zhang, Y. Qiu, Renew. Sustain. Energy Rev. 81 (2018) 1825–1858.
[42] K. Khoshnevisan, H. Maleki, H. Samadian, S. Shahsavari, M.H. Sarrafzadeh, B. Larijani, et al., Carbohydr. Polym. 198 (2018) 131–141.
[43] S. Wang, L. Yi, Y. Fang, L. Wang, J. Yao, J. Marek, et al., J. Appl. Polym. Sci. 138 (2021).
[44] L. Yi, S. Wang, L. Wang, J. Yao, J. Marek, M. Zhang, J. Appl. Polym. Sci. 138 (2021).
[45] Y. Lu, X. Xiao, J. Fu, C. Huan, S. Qi, Y. Zhan, et al., Chem. Eng. J. 355 (2019) 532–539.
[46] S. Wang, W. Chen, L. Wang, J. Yao, G. Zhu, B. Guo, et al., Chemistry (2022).
[47] S.K. Nataraj, K.S. Yang, T.M. Aminabhavi, Prog. Polym. Sci. 37 (2012) 487–513.
[48] L. Zhang, A. Aboagye, A. Kelkar, C. Lai, H. Fong, J. Mater. Sci. 49 (2014) 463–480.
[49] T.-T. Li, Y. Wang, H.-K. Peng, X. Zhang, B.-C. Shiu, J.-H. Lin, et al., Compos. Part A 128 (2020).
[50] R. Zhang, Y. Ma, W. Lan, D.E. Sameen, S. Ahmed, J. Dai, et al., Ultrason. Sonochem. 70 (2021).
[51] P. Duan, Q. Xu, S. Shen, Y. Zhang, X.J.F. Liu, Polymers 20 (2019) 1803–1811.
[52] G. Luo, G. Xi, X. Wang, D. Qin, Y. Zhang, F. Fu, X.J.J.o.A.P.S. Liu, (2017).
[53] R.K. Bhawana, H.S. Basniwal, V.K. Buttar, N.J. Jain, J. Agric. Food. Chem. 59 (2011) 2056–2061.